© 2018. Published by The Company of Biologists Ltd | Development (2018) 145, dev165381. doi:10.1242/dev.165381

RESEARCH ARTICLE

Development of migrating tendon-bone attachments involves replacement of progenitor populations

Neta Felsenthal[1], Sarah Rubin[1], Tomer Stern[1], Sharon Krief[1], Deepanwita Pal[2], Brian A. Pryce[2], Ronen Schweitzer[2] and Elazar Zelzer[1,*]

ABSTRACT

Tendon-bone attachment sites, called entheses, are essential for musculoskeletal function. They are formed embryonically by *Sox9*+ progenitors and continue to develop postnatally, utilizing *Gli1* lineage cells. Despite their importance, we lack information on the transition from embryonic to mature enthesis and on the relation between *Sox9*+ progenitors and the *Gli1* lineage. Here, by performing a series of lineage tracing experiments in mice, we identify the onset of *Gli1* lineage contribution to different entheses. We show that *Gli1* expression is regulated embryonically by SHH signaling, whereas postnatally it is maintained by IHH signaling. During bone elongation, some entheses migrate along the bone shaft, whereas others remain stationary. Interestingly, in stationary entheses *Sox9*$^+$ cells differentiate into the *Gli1* lineage, but in migrating entheses this lineage is replaced by *Gli1* lineage. These *Gli1*$^+$ progenitors are defined embryonically to occupy the different domains of the mature enthesis. Overall, these findings demonstrate a developmental strategy whereby one progenitor population establishes a simple embryonic tissue, whereas another population contributes to its maturation. Moreover, they suggest that different cell populations may be considered for cell-based therapy of enthesis injuries.

KEY WORDS: Musculoskeletal development, Enthesis, Sox9, Gli1, Progenitor cell, Hedgehog signaling, R26R-Confetti, Mouse

INTRODUCTION

The proper assembly of the musculoskeletal system is essential for the function, form and stability of the organism. During embryogenesis, an attachment between tendon and bone, known as an enthesis, is formed. Thereafter, and into the postnatal period, the rudimentary enthesis further develops into a more complex tissue. Although some knowledge on enthesis formation and maturation exists, far less is known about the processes that transform the simple embryonic enthesis into the structure of the mature enthesis.

Traditionally, entheses are divided into either fibrous or fibrocartilaginous, according to their cellular composition. Fibrous entheses form at the attachment site of a tendon that is inserted directly into the bone shaft, forming a structure that resembles a root system. This structure, which is composed of a dense connective tissue (Doschak and Zernicke, 2005; Shaw and Benjamin, 2007; Wang et al., 2013), has been shown to be regulated by parathyroid hormone-like hormone (PTHLH, also known as PTHrP) (Wang et al., 2013). Fibrocartilage entheses typically form at attachment sites of tendons to the epiphysis or to bone eminences. Relative to fibrous entheses, fibrocartilage entheses are structurally more complex, displaying a cellular gradient that is typically divided into four zones, namely tendon, fibrocartilage, mineralized fibrocartilage and bone. The graded tissue, which develops postnatally, dissipates the stress that forms at the attachment site, thereby providing the enthesis with the mechanical strength necessary to withstand compression (Benjamin et al., 2006).

Enthesis development is initiated by the specification of a specialized pool of progenitor cells that express both SRY-box 9 (*Sox9*), a key regulator of chondrogenesis, and the tendon marker scleraxis (*Scx*) (Akiyama et al., 2005; Blitz et al., 2013; Schweitzer et al., 2001; Sugimoto et al., 2013). Cell lineage studies have shown that *Sox9*-expressing progenitor cells contribute to the formation of the enthesis in neonatal mice (Akiyama et al., 2005; Soeda et al., 2010). Another marker for enthesis cells is GLI-Kruppel family member GLI1 (*Gli1*; Liu et al. 2012), a component of the hedgehog (HH) signaling pathway. Lineage studies revealed that *Gli1*-expressing cells act as progenitors that contribute to the formation of some adult entheses (Dyment et al., 2015; Schwartz et al., 2015). However, the relationship between progenitors of the embryonic enthesis and *Gli1* lineage cells, which contribute to the mature enthesis, has not been determined.

The relative position of an enthesis along the bone directly affects its mechanical function and, subsequently, the animal's mobility (Polly, 2007; Salton and Sargis, 2009). Recently, it was shown that all entheses maintain their relative position during bone elongation (Stern et al., 2015). Unlike entheses located at the bone ends, from which the bone elongates, entheses that are located between the epiphyseal plates must maintain their positions during growth. This was shown to occur through either regulation of the relative growth rates at the two epiphyseal plates, or active migration by continuous reconstruction, a process known as bone modeling or drift (Benjamin and McGonagle, 2009; Dörfl, 1980a,b). The latter (referred to hereafter as migrating entheses) encounters a unique developmental challenge. Unlike most organs and tissues, entheses must develop into a complex graded tissue while constantly drifting. This raises the issue of whether the descendants of the embryonic enthesis progenitors continue to serve as the building blocks during maturation of migrating entheses.

In this work, we identify the embryonic stage at which *Gli1* lineage is initiated and demonstrate its contribution to the postnatal enthesis. We show that embryonic *Gli1* expression is initially under the regulation of sonic hedgehog (SHH). Later during postnatal development, Gli1 expression is maintained by Indian hedgehog (IHH). Moreover, we show that *Sox9* lineage does not contribute to

[1]Department of Molecular Genetics, Weizmann Institute of Science, Rehovot 76100, Israel. [2]Research Division, Shriners Hospital for Children, Portland, OR 97201, USA.

*Author for correspondence (eli.zelzer@weizmann.ac.il)

N.F., 0000-0003-4927-7679; T.S., 0000-0003-4279-3558; R.S., 0000-0002-7425-5028; E.Z., 0000-0002-1584-6602

Received 7 March 2018; Accepted 16 November 2018

Development (2018) 145, dev165381. doi:10.1242/dev.165381

postnatal migrating entheses. Instead, *Gli1* lineage cells replace the *Sox9* lineage cells and populate the enthesis. Finally, we show that embryonic *Gli1* lineage cells are pre-determined to contribute to the different layers of the fibrocartilaginous enthesis.

RESULTS

Some entheses undergo cellular and morphological changes during migration

The development of the rudimentary embryonic attachment site into the complex structure of a mature enthesis has received little attention (Galatz et al., 2007). As mentioned, in addition to substantial cellular and morphological changes, some entheses also migrate considerable distances along the bone during bone growth (Benjamin and McGonagle, 2009; Dörfl, 1980a,b; Stern et al., 2015). Therefore, to study the transition that migrating entheses undergo during maturation, we documented morphological and molecular changes, as well as drifting activity, in entheses from embryonic day (E) 14.5 to postnatal day (P) 14. We focused on two migrating entheses, namely the deltoid enthesis (DT), a fibrocartilaginous enthesis that forms between the deltoid tendon and the deltoid tuberosity, and the teres major enthesis (TM), a fibrous enthesis that forms between the teres major tendon and the humeral shaft.

Analysis of enthesis positions during development revealed that both DT (0.778±0.026 mm, data are mean±s.d.) and TM (1.624±0.171 mm) entheses drifted considerably along the bone shaft during bone elongation (Fig. 1A). Histological sections through wild-type (WT) mouse humeri showed that both embryonic entheses displayed a simple structure of layered cells (Fig. 1B,Ca,Da). However, the overall shape of the enthesis changed dramatically throughout development, as it protruded outwards from the bone shaft and the different enthesis domains became more noticeable (Fig. 1Ca′-Ca‴,Da′-Da‴). Tissue complexity also increased, as a larger variety of cells, such as fibrocartilage cells and osteoblasts (Benjamin and McGonagle, 2009), were identified along with an increase in extracellular matrix (Fig. 1Cd,Cd′,Ch,Ch′,Dd,Dd′,Dh,Dh′). The increased complexity was also demonstrated by a change in the expression patterns of structural genes, such as bone sialoprotein (*Bsp*; also known as integrin binding sialoprotein, *Ibsp*), collagen type 2 alpha 1 (*Col2a1*), collagen type 12 alpha 1 (*Col12a1*) and tenascin C (*Tnc*), and regulatory genes such as *Gli1*. Furthermore, expression domains correlating to various structural domains emerged, namely *Col12a1*, *Tnc*, *Gli1* and *Col1a1* in tendon and fibrocartilage (Fig. 1Cc,Cf-Ch, Dc,Df-Dh), and *Col1a1*, *Gli1* and *Bsp* in mineralized fibrocartilage and bone (Fig. 1Cc,Ce,Ch,Dc,De,Dh).

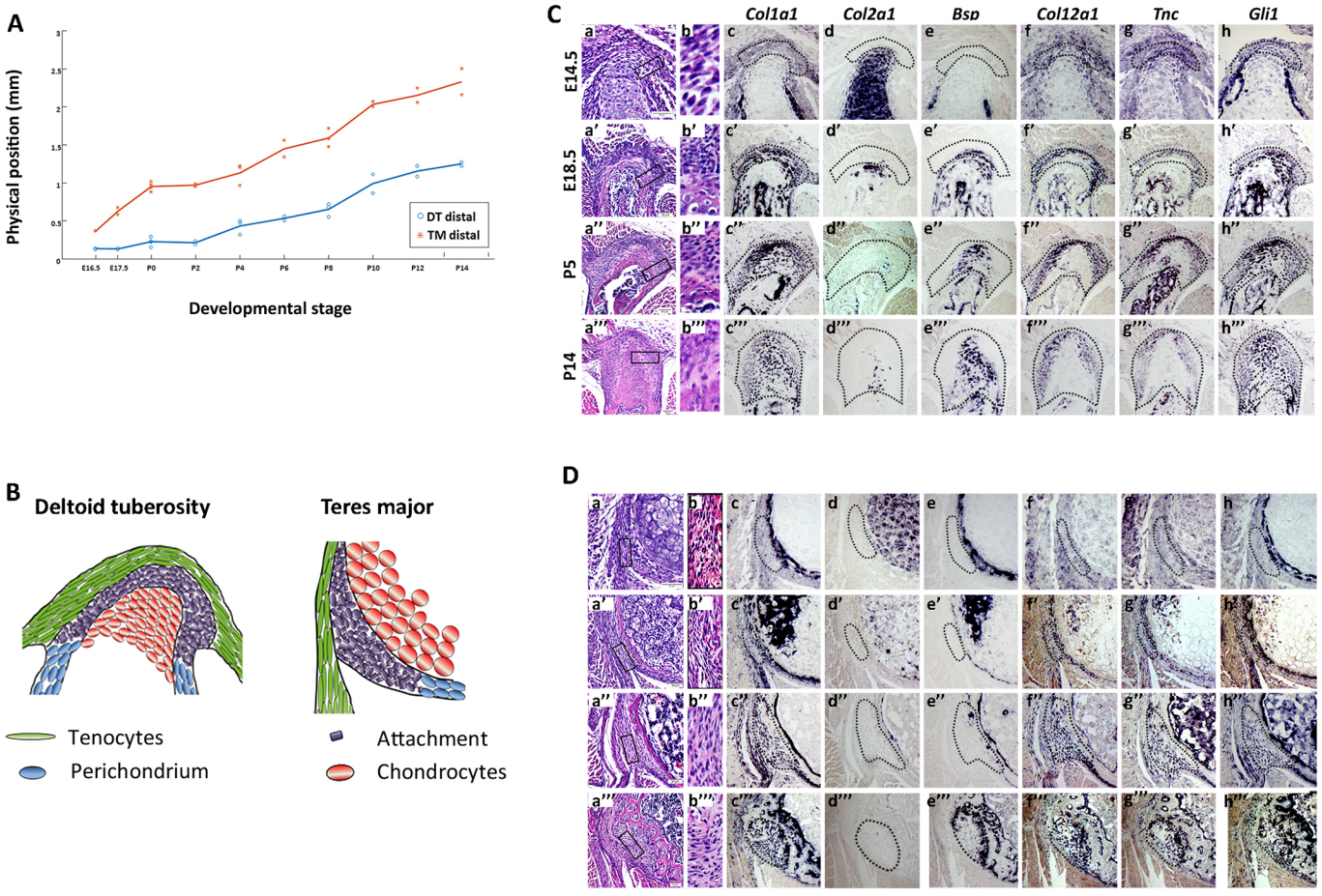

Fig. 1. Some entheses undergo cellular and morphological changes while migrating. (A) Graph showing the physical position of the DT and TM entheses along the bone throughout development (E16.5-P14), defined as the distance of the element (mm) from a predefined longitudinal origin roughly at the center of the shaft. Positive and negative values correspond to elements that are proximal and distal to the point of origin, respectively. As indicated by the steep slope of the curves, both DT and TM migrate considerably throughout development. (B) Schematics of the embryonic DT and TM entheses. (C,D) Transverse sections through the humerus showing the DT (C) and TM (D) entheses of E14.5-P14 WT mice. (Ca,Cb,Da,Db) H&E staining. Cb and Db are magnifications of the boxed areas in Ca and Da, respectively. (Cc-Ch,Dc-Dh) ISH using DIG-labeled, anti-sense complementary RNA probes for *Col1a1*, *Col2a1*, *Bsp*, *Col12a1*, *Tnc* and *Gli1* at E14.5 (c-h), E18.5 (c′-h′), P5 (c″-h″) and P14 (c‴-h‴). Dotted line demarcates the enthesis. Scale bars: 50 µm.

Development (2018) 145, dev165381. doi:10.1242/dev.165381

Gli1^{+} cell lineage contributes to the postnatal enthesis

Lineage tracing experiments have shown that *Gli1* lineage cells contribute to postnatal enthesis development (Dyment et al., 2015; Schwartz et al., 2015). Yet, the onset of this lineage during embryogenesis and its dynamics in different entheses have been missing. In order to identify the onset of *Gli1* lineage, we performed pulse-chase experiments on *Gli1-CreER*^{T2} mice (Ahn and Joyner, 2004) crossed with *R26R-tdTomato* reporter mice (Madisen et al., 2010), which allowed us to mark *Gli1*-expressing cells at specific time points and follow their descendants. We analyzed three entheses that represented different types, namely DT (migratory-fibrocartilaginous), TM (migratory-fibrous) and Achilles (stationary-fibrocartilaginous). Examination of neonatal (P0) TM and DT entheses following tamoxifen administration at E9.5-E12.5 revealed only a few *Gli1* lineage cells (Fig. 2Aa-Da,Ab-Db). However, administration at E13.5 and E15.5 resulted in extensive labeling in both migratory entheses (Fig. 2Ea,Eb,Fa,Fb). In the stationary Achilles enthesis, we observed labeled cells in tendon and cartilage at P0 following tamoxifen administration at E9.5-E10.5 (Fig. 2Ac,Bc); yet, tamoxifen administration at later time points (E11.5-E14.5) did not result in labeled cells (Fig. 2Cc,Dc,Ec). Tamoxifen administration at E15.5 labeled cells specifically in the enthesis and perichondrium and not in adjacent cartilage (Fig. 2Fc). Although we cannot rule out periodic expression of *Gli1* in the Achilles enthesis cells, it is possible that the early labeling represents a direct readout of HH expression in the zone of polarizing activity (Ahn and Joyner, 2004), whereas the later expression is a specific induction of *Gli1* in enthesis cells. The postnatal contribution of *Gli1* lineage to migratory entheses was further established by following E13.5 lineage induction to P14 (Fig. 2Ga-Gc). Together, these results indicate that, although *Gli1* lineage is not induced at the onset of enthesis formation (Blitz et al., 2013; Sugimoto et al., 2013), it contributes differentially to different entheses during embryonic development.

Gli1 expression in migrating entheses is initiated by SHH and maintained by IHH

It has previously been suggested that the HH signaling pathway plays a role in regulating the activity of *Gli1*$^{+}$ enthesis cells (Breidenbach et al., 2015; Dyment et al., 2015; Liu et al., 2013; Schwartz et al., 2015). Therefore, our finding that *Gli1* expression is initiated at early stages of enthesis development (Fig. 1Ch,Dh) raised the issue of which component of the HH pathway regulates *Gli1* expression in enthesis cells and whether it also affects migratory entheses. It was suggested that IHH, an effector of the HH signaling pathway, is a possible regulator of *Gli1* lineage cells in adult stationary entheses. In order to examine the possible role of IHH in inducing *Gli1* expression in the embryonic enthesis, we blocked *Ihh* expression in the limb by using *Prx1-Cre-Ihh*$^{-/-}$ mice. Interestingly, at E14.5 *Gli1* was expressed in control and mutant entheses, suggesting that IHH is not necessary for *Gli1* induction in embryonic enthesis progenitors (Fig. 3A,A′). We therefore examined the possible role of another regulator of HH signaling, SHH, by analyzing the *Gli1* expression of embryonic enthesis cells in *Shh* KO embryos (*Shh-GFPCre*$^{-/-}$). Results showed that *Gli1* expression dramatically decreased in the mutant entheses compared with the WT (Fig. 4C-D′), suggesting that SHH is necessary for the induction of *Gli1* in embryonic enthesis cells.

That result was intriguing, because we observed that *Gli1* was constantly expressed by both embryonic and postnatal enthesis cells (Fig. 1Ah-Ah‴,Bh-Bh‴), whereas *Shh* is expressed in the limb only during embryogenesis (Harfe et al., 2004). This raised the issue of how *Gli1* expression in the enthesis is maintained after the loss of *Shh* expression. To address the possibility that *Ihh* controls *Gli1* expression in the postnatal enthesis, even though it is not involved in the induction of *Gli1* expression in embryonic enthesis progenitors, we analyzed *Prx1-Cre-Ihh*$^{-/-}$ mice at P10. Results showed that, although *Gli1* expression was maintained in mutant muscle and bone, in the enthesis it was completely lost (Fig. 3B,B′), which indicates that *Ihh* is indeed required for the maintenance of *Gli1* expression in enthesis cells. To identify the source of *Ihh* in the enthesis, we performed immunofluorescence staining for IHH protein in P6 enthesis sections. As seen in Fig. 3 (C-F), IHH was highly expressed in mineralized fibrocartilage and bone regions at the enthesis center, along with its expression in surrounding muscles. Taken together, these results suggest that *Gli1* expression by embryonic enthesis progenitors is induced by SHH and later, in

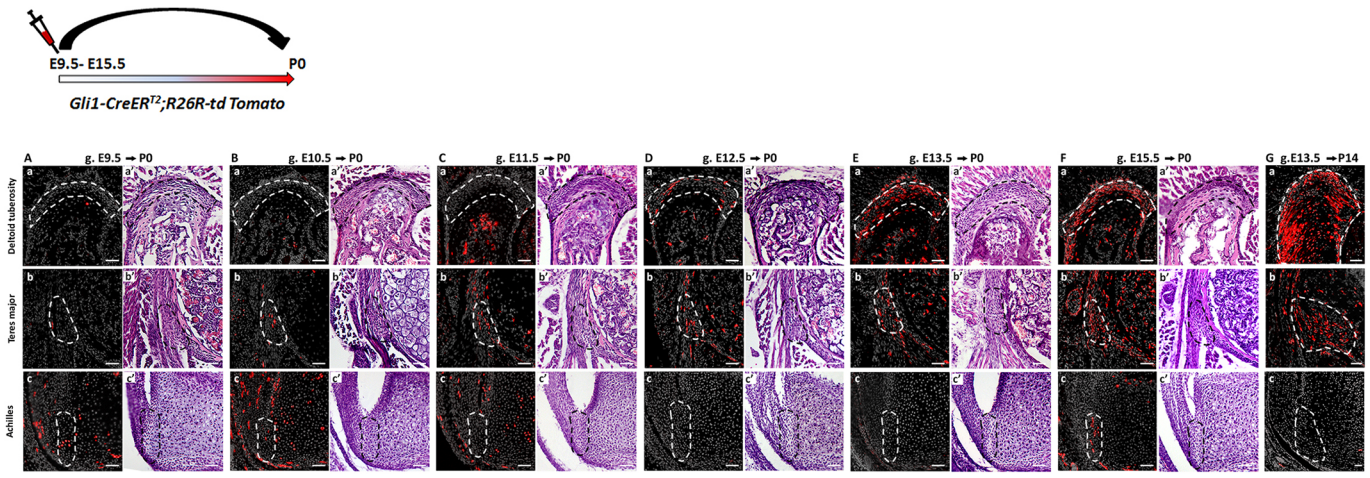

Fig. 2. *Gli1*$^{+}$ cell lineage contributes to the postnatal enthesis. (A-G) Pulse-chase cell lineage experiments using *Gli1-CreER*^{T2}*;R26R-tdTomato* mice demonstrate the contribution of *Gli1* lineage cells to various entheses. *Gli1*$^{+}$ cells were labeled by a single tamoxifen administration at different time points (E9.5-E15.5) and their descendants were followed to P0 and P14. (Aa-Fa) The DT enthesis was extensively marked after tamoxifen administration at E13.5 and E15.5. (Ab-Fb) tdTomato^{+} cells were identified in the TM enthesis starting at E10.5; however, a stronger signal was seen following tamoxifen administration at E13.5 or later. (Ac-Fc) tdTomato^{+} cells were identified in the Achilles tendon enthesis following tamoxifen administration at E9.5 and E15.5. On the right of each image, a corresponding H&E section shows the enthesis region. (Ga-Gc) Both DT and TM, but not the Achilles entheses, were extensively marked at P14 following tamoxifen administration at E13.5. Dashed line demarcates the enthesis. Scale bars: 50 µm.

Development (2018) 145, dev165381. doi:10.1242/dev.165381

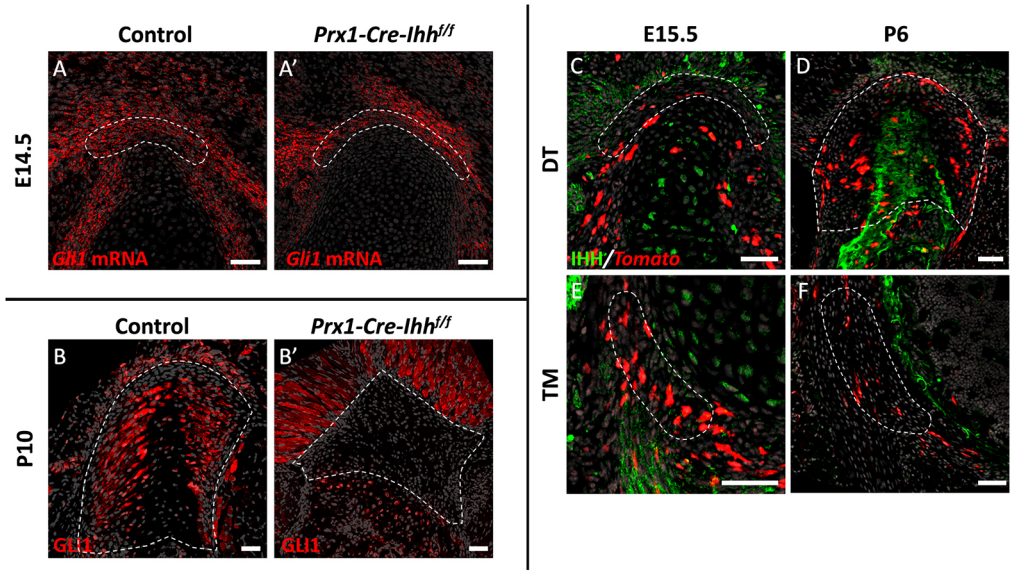

Fig. 3. *Gli1* expression in the enthesis is maintained by IHH. (A,A′) Fluorescent ISH for *Gli1* on sections through the DT of E14.5 control (A) and *Prx1-Cre-Ihh*$^{f/f}$ embryos (A′) demonstrates that, in the absence of IHH signaling, *Gli1* expression in the enthesis remains similar. (B,B′) Immunostaining for GLI1 protein in P10 control (B) and *Prx1-Cre-Ihh*$^{f/f}$ (B′) DT sections shows that, in the absence of IHH, GLI1 protein expression is lost from the DT enthesis. (C-F) Immunostaining for IHH protein in *Gli1-CreER*^{T2}*;R26R-tdTomato* DT (C,D) and TM (E,F) entheses. Tamoxifen was administered at E13.5 and mice were sacrificed at E15.5 (C,E) or P6 (D,F). IHH expression is seen in hypertrophic chondrocytes at E15.5 and in the mineralizing part of the enthesis at P6. IHH is also expressed in surrounding muscle at E15.5. Dashed line demarcates the enthesis. Scale bars: 50 µm.

the maturing enthesis, maintained by IHH that originates in mineralized fibrocartilage and bone.

Sox9 lineage cells of the embryonic enthesis do not contribute to postnatal migrating entheses

The embryonic enthesis originates from *Scx*$^{+}$/*Sox9*$^{+}$ progenitor cells (Blitz et al., 2013; Sugimoto et al., 2013). Yet, the contribution of these progenitors to the postnatal enthesis and their relation to the *Gli1* lineage cells have never been studied. To fill this gap, we first examined the contribution of *Sox9* lineage to the postnatal enthesis. To that end, we performed a pulse-chase cell lineage experiment using mice that express Cre-ER under control of the *Sox9* promoter (*Sox9-CreER*^{T2}) crossed with *R26R-tdTomato* reporter mice (Soeda et al., 2010). It has previously been demonstrated that tamoxifen administration at E12.5 effectively labels embryonic enthesis cells (Blitz et al., 2013; Soeda et al., 2010). Indeed, examination at P0 following tamoxifen administration at E12.5 showed that the DT, TM and Achilles entheses were populated by tdTomato^{+} cells, which suggests that, at that stage, the enthesis is populated by *Sox9* lineage cells (Fig. 5Aa-Ac). Yet, surprisingly, at P14 we observed a dramatic decrease in the contribution of tdTomato-expressing cells to the two migrating entheses (Fig. 5Aa′,Ab′,Ad), although the cells in the stationary enthesis and in the humerus were still extensively labeled (Fig. 5Ac′,Ad). These results suggest that postnatal stationary enthesis cells were descendants of the *Sox9*$^{+}$ embryonic lineage, whereas in migrating entheses this lineage was lost.

The labeled stationary entheses could serve as a positive internal control for the effectiveness of labeling. Nevertheless, to rule out the possibility that tamoxifen was administered at the wrong time point, we repeated the experiment while administering tamoxifen at different time points from E11.5 to E17.5 (Fig. 5B). Examination at P14 showed minimal contribution of *Sox9* lineage cells to the postnatal entheses, similar to the results obtained following pulsing at E12.5. Taken together, these results indicate that the embryonic *Sox9* lineage contributes poorly to postnatal migrating entheses, suggesting that these entheses are populated by another cell lineage postnatally.

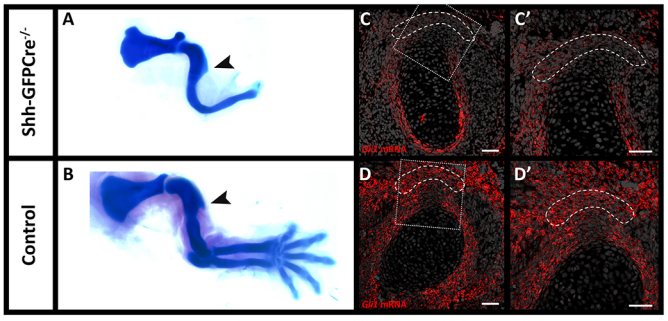

Fig. 4. *Gli1* expression in the enthesis is initiated by SHH. (A,B) Skeletal preparations from control and *Shh-GFPCre*$^{-/-}$ embryos at E14.5 demonstrate that, although limb morphology is greatly impaired in the mutant, proximal humerus morphology remains similar and the DT is formed. Arrowheads indicate the deltoid tuberosity. (C-D′) Fluorescent ISH for *Gli1* mRNA on sections through the DT of E14.5 *Shh-GFPCre*$^{-/-}$ (C-C′) and control (D-D′) embryos show that, in the absence of SHH signaling, *Gli1* mRNA and expression in the DT enthesis is lost. C′ and D′ are magnifications of the boxed areas in C and D, respectively. Dashed line demarcates the enthesis. Scale bars: 50 µm.

Gli1 lineage cells replace the embryonic *Sox9* lineage during enthesis maturation

Our finding that both embryonic *Gli1* and *Sox9* lineages contribute to the stationary postnatal enthesis suggests that these two genes mark a common cell lineage. Conversely, the finding that embryonic *Sox9* lineage contributes to embryonic but not to postnatal migrating enthesis implies that, postnatally, embryonic *Gli1* lineage replaces the *Sox9* lineage to form the mature enthesis.

Development (2018) 145, dev165381. doi:10.1242/dev.165381

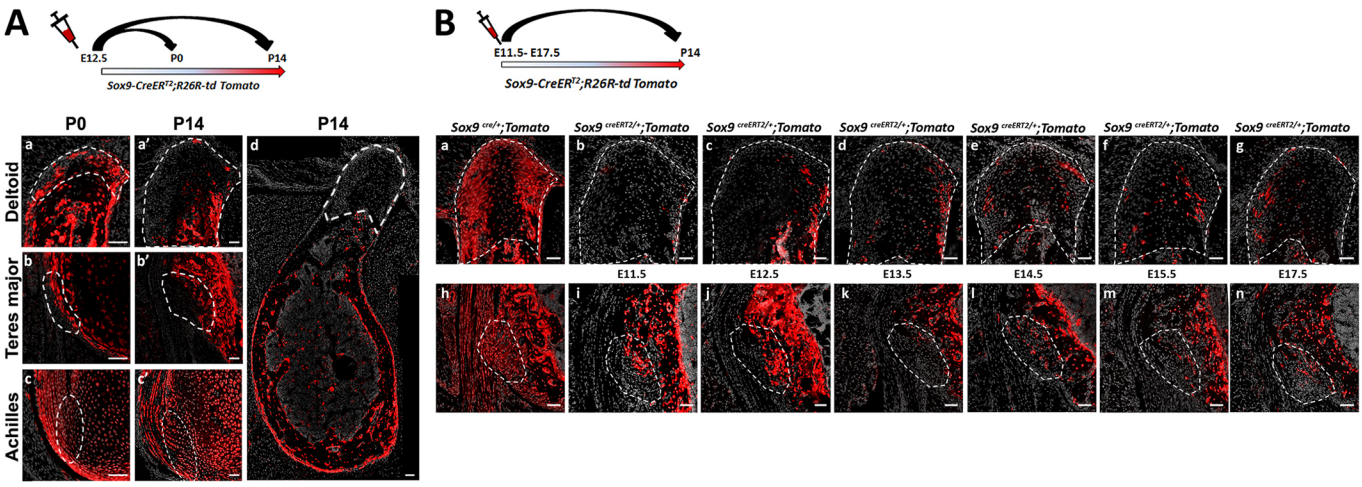

Fig. 5. *Sox9* lineage cells of the embryonic enthesis do not contribute to postnatal migrating entheses. (A) Pulse-chase cell lineage experiment using *Sox9-CreER^{T2};R26R-td Tomato* mice demonstrates that *Sox9* lineage contributes differently to migrating and to stationary entheses. *Sox9*$^+$ cells were marked at E12.5 by a single tamoxifen administration. At P0, tdTomato$^+$ cells were identified in migrating DT and TM entheses (Aa,Ab) as well as in stationary Achilles entheses (Ac). At P14, only a few tdTomato$^+$ cells were identified in migrating entheses (Aa′,Ab′,Ad), whereas extensive staining was still seen in stationary entheses (Ac′) and in other areas of the bone, as seen in a section through the humerus in Ad. (B) The contribution of *Sox9* lineage to the DT and TM entheses was evaluated by crossing *Sox9-Cre* or *Sox9-CreER^{T2}* mice with *R26R-tdTomato* reporter mice. (Ba,Bh) The total contribution of the lineage was evaluated by examination of *Sox9-Cre;R26R-tdTomato* mice at P14. (Bb-Bg,Bi-Bn) The relative contribution of *Sox9* lineage cells specified at different time points was evaluated by pulse-chase experiments on *Sox9-CreER^{T2};R26R-tdTomato* mice, in which a single dose of tamoxifen was administered at various stages from E11.5 through E17.5. Dashed line demarcates the enthesis. Scale bars: 50 µm.

To study the process of lineage replacement and to follow its dynamics, we traced both lineages throughout enthesis development, from E15.5 to maturation at P14, by pulse-chase experiments. As seen in Fig. 6, at E15.5 and P0 in both the DT and TM, *Sox9* lineage cells populated the embryonic enthesis. However, from P0 their number decreased dramatically and, by P8, the enthesis contained only a limited number of these cells. Concurrently, the number of cells of the *Gli1* lineage gradually increased in both entheses and, by P8, *Gli1*$^+$ cells inhabited most of the enthesis structure. Interestingly, the gradual population of the DT and TM entheses by *Gli1* lineage cells correlated with the temporal dynamics of enthesis migration (Fig. 1A). These results support our hypothesis that, during early postnatal development of migrating entheses, a new population that is derived from *Gli1*$^+$ progenitors substitutes the *Sox9* lineage cells of the embryonic enthesis.

Cellular mechanism that underlies the elimination of Sox9 lineage cells in migrating entheses

The loss of *Sox9*$^+$ lineage cells during the replacement process raised the issue of the mechanism that underlies their disappearance from the enthesis. Several mechanisms could account for the elimination of these cells, including bone modeling by osteoclasts, cell death and phagocytosis. To decide between these options, we analyzed P6 and P4 *Sox9-CreER;tdTomato* mouse humeri following tamoxifen administration at E12.5. We first traced the presence of osteoclasts using TRAP staining. As seen in Fig. 7, we identified TRAP$^+$ cells at the enthesis in proximity to *Sox9*$^+$ lineage cells, which suggests that Sox9-lineage elimination is performed, at least in part, by bone modeling. Next, we addressed the possibility of apoptosis by TUNEL assay. As seen in Fig. 8, we identified TUNEL$^+$ cells in both entheses, which suggests that cell death might contribute to the cell lineages replacement process. Finally, we examined the presence of phagocytic cells that could eliminate *Sox9*$^+$ lineage cells using F4/80 antibody staining. Results showed a few F4/80$^+$ cells in proximity to *Sox9*$^+$ lineage cells, suggesting that they too participate in *Sox9*$^+$ lineage elimination (Fig. 9). Altogether, these results suggest that *Sox9*$^+$ cells are eliminated by a combination of different mechanisms, including bone modeling, cell death and phagocytosis.

Gli1$^+$ progenitors are compartmentalized during embryonic enthesis development

The increasing cellular complexity of the developing enthesis, and our finding that progenitors of the *Gli1* lineage that will contribute to the postnatal enthesis are already present during embryonic development, led us to ask whether these progenitors are already assigned to a specific domain within the forming enthesis; for example, fibrocartilage or mineralized fibrocartilage. To study this possibility, we conducted pulse-chase experiments on *Gli1-CreER^{T2}* mice crossed with *R26R-Confetti* mice (Snippert et al., 2010) that, upon recombination, stochastically express GFP, RFP, CFP or YFP, allowing for the identification of different cell clones. Finding clones that cross domain boundaries would indicate that there is no compartmentalization of the Gli1 progenitors. Conversely, finding restricted clones would support the existence of embryonic compartmentalization of these cells.

We focused on the two main domains of the DT enthesis, namely mineralized and non-mineralized fibrocartilage, and on the border between entheseal mesenchymal cells and bone in the TM enthesis. Examination of P14 limbs following tamoxifen administration at E13.5 revealed multiple clones in both entheses, most of which were restricted to a specific domain (Fig. 10). These results suggest that at E13.5, the *Gli1* lineage progenitors are already assigned a specific enthesis domain.

DISCUSSION

The transition from the embryonic to the mature enthesis has been understudied. Here, we use genetic lineage tracing to unravel the cellular developmental sequence of fibrous and fibrocartilaginous entheses. We show that, although *Gli1*$^+$ progenitors contribute to entheses of both types, their contribution differs greatly between

Development (2018) 145, dev165381. doi:10.1242/dev.165381

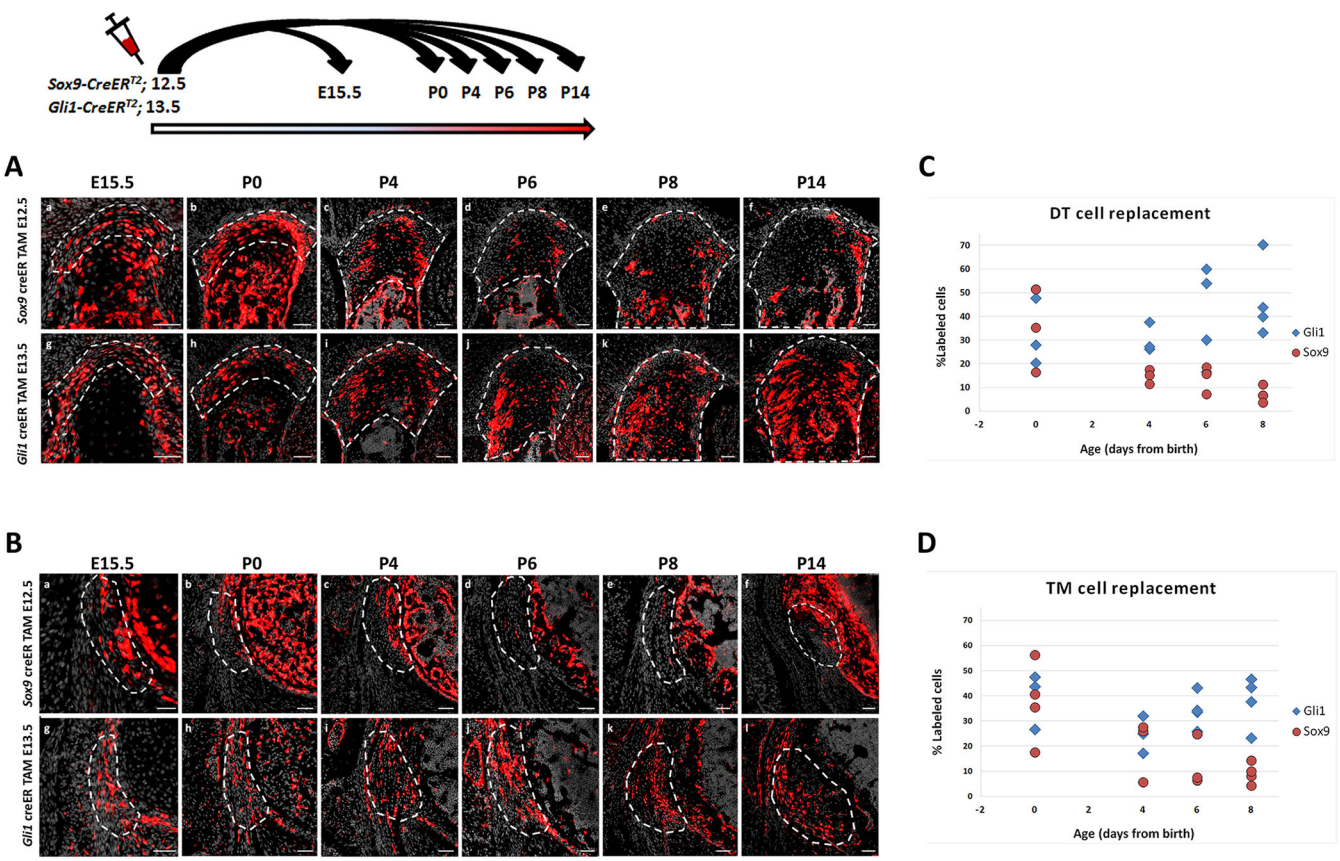

Fig. 6. *Gli1* lineage cells replace *Sox9* lineage cells during entheses maturation. (A,B) *Sox9-CreER^{T2};R26R-tdTomato* and *Gli1-CreER^{T2};R26R-tdTomato* mice were labeled by tamoxifen administration at E12.5 and E13.5, respectively, and sacrificed at E15.5-P14. Transverse sections through the DT (A) and TM (B) show an increase in *Sox9* lineage cells at E15.5-P0. Between P0 and P14, a continuous decrease in *Sox9* lineage cells is seen. Concurrently, *Gli1* lineage cell number gradually increased in both DT and TM entheses. By P8, both entheses were populated by *Gli1* lineage cells. (C,D) The percentages of *tdTomato*$^{+}$ cells in *Sox9-CreER^{T2};R26R-tdTomato* and *Gli1-CreER^{T2};R26R-tdTomato* limbs were significantly different in the DT (C, P=0.0010) and TM (D, P=0.0019). Additionally, there was a significant decrease in the percentage of *tdTomato*$^{+}$ cells in *Sox9-CreER^{T2};R26R-tdTomato* limbs over time (P=0.020). Dashed line demarcates the enthesis. Scale bars: 50 µm.

stationary and migratory entheses. In stationary entheses, *Gli1*$^{+}$ progenitors are descendants of *Sox9*$^{+}$ progenitors that have established the embryonic enthesis. However, in migrating entheses, a separate, compartmentalized population of *Gli1*$^{+}$ progenitors is recruited to the embryonic enthesis, co-populates it alongside *Sox9*$^{+}$ progenitors and, eventually, replaces them during postnatal development.

As mentioned, fibrous and fibrocartilaginous entheses exhibit marked differences in structure and composition (Benjamin et al., 2002). Notwithstanding the importance of this distinction, the observed differences in cellular origin between stationary and migrating entheses calls for a revision of the traditional classification and suggests that it should be taken into account whether an enthesis is ‘migratory’ or ‘stationary’.

Organ development can be mediated by several cellular mechanisms. In a linear mechanism, an embryonic set of progenitors forms a primordium and then continues to proliferate and differentiate to form the mature organ. Another mechanism is cell recruitment, during which cells are supplied to the forming organ after primordium establishment. A third mechanism involves template replacement, in which an initial template is formed by one type of cells to be later replaced by another cell population, which will form the mature organ. Interestingly, in the musculoskeletal system there are examples of all these modes of development. Muscles and joints develop through cell recruitment (Buckingham et al., 2003; Shwartz et al., 2016), whereas most of the skeleton develops through template replacement, namely by endochondral ossification (Kronenberg, 2003). Here, we show that stationary entheses develop linearly by embryonic *Sox9*$^{+}$ progenitors that form the postnatal enthesis and later upregulate the expression of *Gli1*. However, we show that migrating entheses develop through template replacement, as *Gli1*$^{+}$ progenitors replace the *Sox9*$^{+}$ embryonic enthesis cells and form the mature enthesis.

Previous studies have shown not only that *Gli1* is a marker for the forming enthesis, but that the HH pathway plays an active role in regulating enthesis maturation and regeneration (Breidenbach et al., 2015; Dyment et al., 2015; Liu et al., 2013; Schwartz et al., 2015, 2017). *Ihh* expression was identified in proximity to the *Gli1*$^{+}$ progenitor population in stationary entheses (Dyment et al., 2015; Liu et al., 2013; Schwartz et al., 2015). Moreover, loss-of-function of *Smo*, a component of the HH pathway, in *Scx*-expressing cells resulted in reduced mineralization of the enthesis (Breidenbach et al., 2015; Dyment et al., 2015; Liu et al., 2013; Schwartz et al., 2015). Yet, the question of which ligand of the HH pathway regulates the specification of *Gli1*$^{+}$ cells in the embryo and, specifically, in migrating enthuses, has remained unanswered. Our results clearly suggest that *Gli1* expression is regulated by both SHH and IHH during enthesis development. In the embryo, we show that SHH, but not IHH, signaling is essential for *Gli1* expression in the enthesis, implicating SHH in *Gli1*$^{+}$ progenitor specification.

Development (2018) 145, dev165381. doi:10.1242/dev.165381

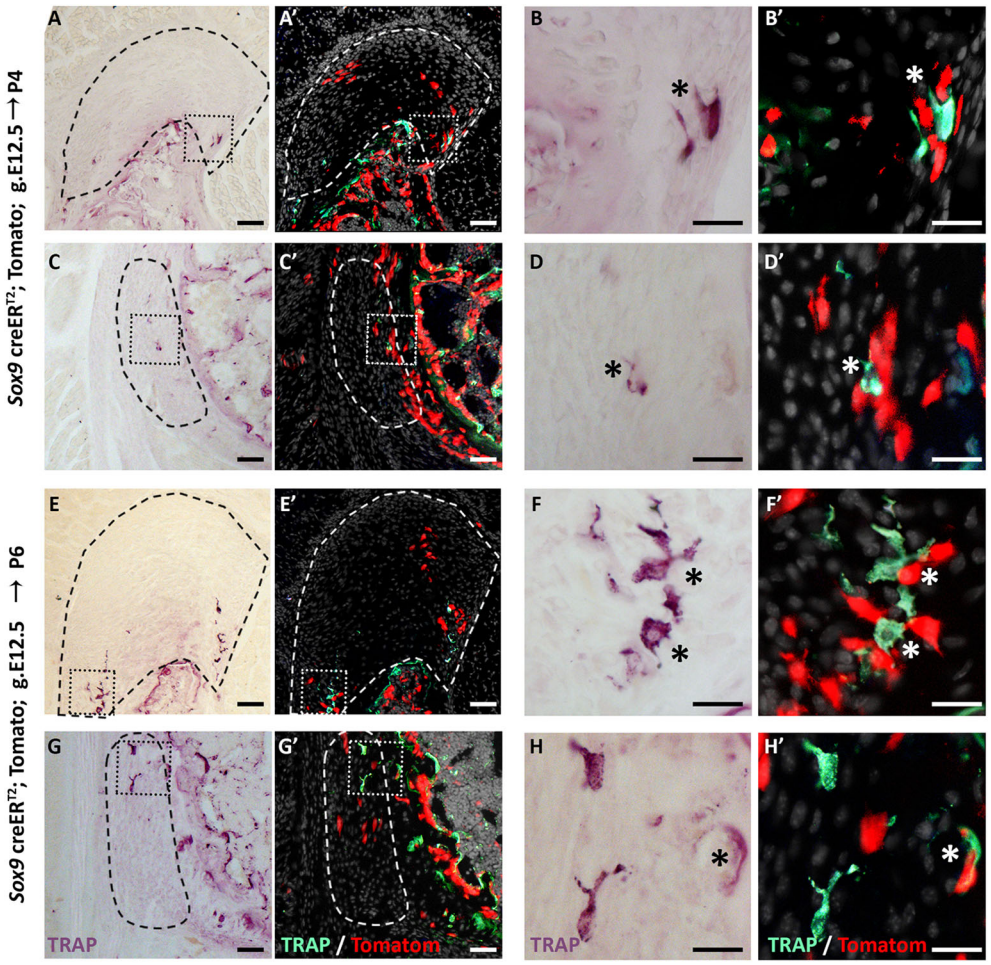

Fig. 7. Close spatial proximity between *Sox9*$^+$ lineage cells and osteoclasts. (A-H′) TRAP staining of P4 and P6 humeri shows osteoclasts (asterisk) in proximity to Sox9$^+$ lineage cells in the DT (A-B′,E-F′) and in the TM (C-D′,G-H′). In A′-H′, TRAP expression images (A,C,E,G) were inverted and overlaid with tdTomato signal from Sox9-CreER;tdTomato lineage cells. B,B′,D,D′,F,F′,H,H′ are magnifications of the boxed areas in A,A′,C,C′,E,E′,G,G′, respectively. Dashed line demarcates the enthesis. Scale bars: 50 µm in A,C,E,G; 20 µm in B,D,F,H.

However, during postnatal development, *Ihh* expression is vital for maintaining *Gli1* enthesis expression.

An obvious concern regarding this conclusion relates to the mispatterning of the *Shh* mutant limb, which might lead to aberrant *Gli1* expression. Although one cannot completely rule out this possibility, the patterning of the mutant's proximal humerus was comparable with that of WT. Thus, it is reasonable to assume that the loss of *Gli1* expression was a direct effect of SHH loss. This suggests that SHH has a specific role in regulating *Gli1* expression in the enthesis.

During endochondral ossification, IHH regulates hypertrophic chondrocyte differentiation and, thereby, bone elongation (Vortkamp et al., 1996). It is therefore possible that, by controlling both these processes, IHH coordinates enthesis migration with the concurrent bone elongation to preserve enthesis position along the shaft. However, the signals that govern enthesis positioning and migration along the bone, including the possible effect of IHH on these processes, are yet to be elucidated.

Another key issue surrounds the mechanism that facilitates the replacement between *Sox9*$^+$ and *Gli1*$^+$ cell populations. Finding evidence for the existence of osteoclasts, phagocytes and cells that are undergoing apoptosis in proximity to *Sox9*$^+$ cells during the replacement process suggests that all of these mechanisms might contribute to *Sox9*$^+$ lineage cell elimination. Yet, none of these findings was compelling enough to provide an explanation for the massive loss of *Sox9*$^+$ cells from the attachment site. Therefore, our results do not rule out other mechanisms for the elimination of *Sox9* lineage cells, including the migration of these cells to other regions in the bone. Moreover, whether the replacement process is the mechanism that allows migrating entheses to maintain their relative position along the bone is yet to be determined.

Finally, our finding that *Gli1*-expressing cells have already been assigned domains in the embryo suggests the existence of an earlier, yet unknown, mechanism that regulates the compartmentalization of these progenitors. It would be interesting to determine whether, besides being compartmentalized, the fate of these cells is also pre-determined or, similar to the neural crest cells (Trainor and Krumlauf, 2000), these cells are multipotent and their fate is determined later by cell-community effect. Resolving these issues may hold therapeutic potential.

To conclude, our findings shed light on developmental linearity in organogenesis. Using the enthesis as a model system, we identified two different strategies of development (Fig. 11). The first, found in stationary entheses, is linear development, in which embryonic progenitors and their descendants contribute to the entire process of enthesis development, from embryogenesis to maturity. Conversely, in migrating entheses, another developmental strategy was identified in which one type of progenitor cells form an embryonic template, only to be later replaced by another cell lineage that contributes to the mature organ.

MATERIALS AND METHODS

Animals

All experiments involving mice were approved by the Institutional Animal Care and Use Committee (IACUC) of the Weizmann Institute. Histology was performed on BL6 mice.

Development (2018) 145, dev165381. doi:10.1242/dev.165381

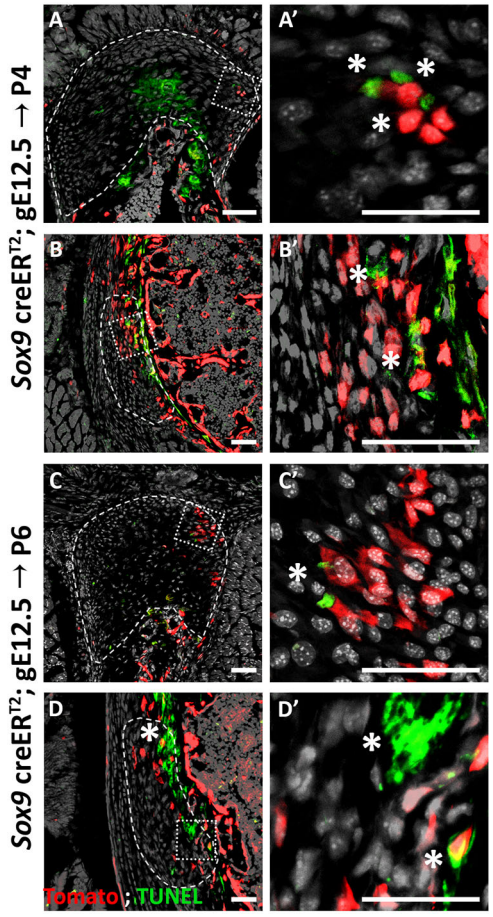

Fig. 8. Some enthesis cells undergo cell death. (A-D′) TUNEL staining of P4 (A,B) and P6 (C,D) humeri show apoptotic cells in the DT (A,C) and in the TM (B,D). E13.5 autopod was used as a control (see Fig. S1). Dashed line demarcates the enthesis; asterisks indicate TUNEL-positive cells. A′,B′,C′,D′ are magnifications of the boxed areas in A,B,C,D, respectively. Scale bars: 50 µm.

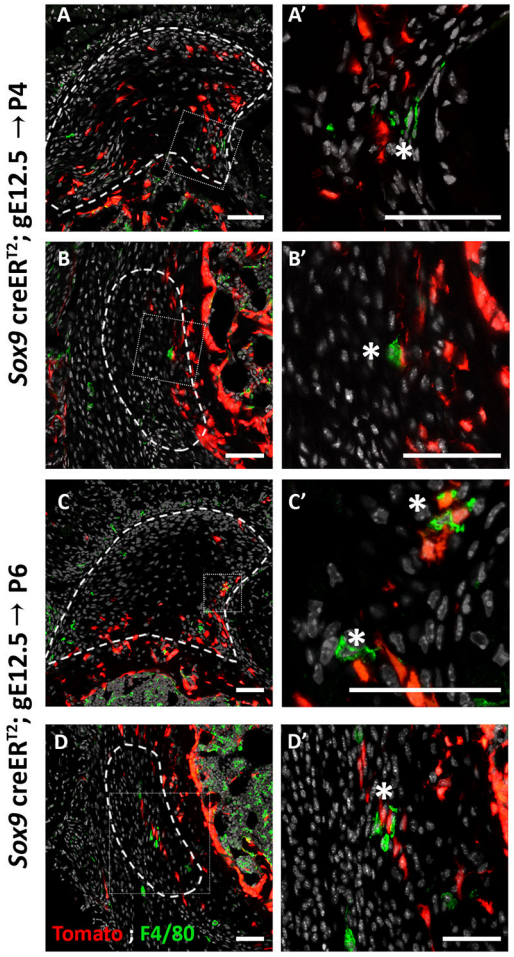

Fig. 9. *Sox9*$^{+}$ lineage cells are in close proximity to phagocytes. (A-D′) F4/80 staining, marking phagocytes, of P4 (A,B) and P6 (C,D) humeri show phagocytic cells (asterisk) proximal to Sox9^{+} lineage cells in the DT (A,A′,C,C′) and in the TM (B,B′,D,D′). A′-D′ are magnifications of the boxed areas in A-D, respectively. Dashed line demarcates the enthesis. Scale bars: 50 µm.

For lineage tracing experiments, *Sox9-Cre* (Akiyama et al., 2005), *Sox9-CreER* (Soeda et al., 2010) and *Gli1-CreER*^{T2} (Ahn and Joyner, 2004; Jackson Laboratory) mice were crossed with *R26R-tdTomato* mice [B6;129S6-*Gt(ROSA)26Sor*$^{tm9(CAG\text{-}tdTomato)Hze}$/J; Madisen et al., 2010] or with *R26R-Confetti* mice [B6.129P2-*Gt(ROSA)26Sor*$^{tm1(CAG\text{-}Brainbow2.1)Cle}$/J; Snippert et al., 2010].

To create *Shh* KO mice, mice heterozygous for a mutation in *Shh* [B6.Cg-*Shh*$^{tm1(EGFP/cre)Cjt}$/J; Jackson Laboratory] were intercrossed; heterozygotes or WT littermates were used as a control. The generation of *Prx1-Cre* (Logan et al., 2002) has been previously described. To generate *Prx1-Cre-Ihh* mutant mice, *Ihh*-floxed mice (B6N;129S4-*Ihh*^{tm1Blan}/J; Jackson Laboratory) (Razzaque et al., 2005) were mated with *Prx1-Cre* mice. As a control, *Prx1-Cre*$^{-}$ animals were used.

For cell lineage experiments, *Sox9-CreER*$^{T2/+}$ or *Gli1-CreER*$^{T2/+}$ males were crossed with *R26R-tdTomato* females to produce embryos carrying both the relevant *CreER*^{T2} and *R26R-tdTomato* alleles. For fate mapping, *Gli1-CreER*$^{T2/+}$ males were crossed with *R26R-Confetti* females to produce embryos carrying both the *Gli1-CreER*^{T2} and *Confetti* alleles.

In all experiments, $n \geq 3$ embryos or mice from different litters. In all timed pregnancies, plug date was defined as E0.5. For harvesting of embryos, timed-pregnant females were sacrificed by cervical dislocation. The gravid uterus was dissected out and suspended in a bath of ice-cold PBS and the embryos were harvested after removal of amnion and placenta. Tail genomic DNA was used for genotyping.

Histological analysis, *in situ* hybridization and immunofluorescence

For histology and *in situ* hybridization (ISH), embryos were harvested at various ages, dissected and fixed in 4% paraformaldehyde (PFA)/PBS at 4°C overnight. After fixation, tissues were dehydrated to 70% EtOH and embedded in paraffin. The embedded tissues were cut to 7-µm-thick sections and mounted onto slides. Hematoxylin and Eosin (H&E) staining was performed following standard protocols. Non-fluorescent and fluorescent ISH was performed as has been previously described using digoxigenin (DIG)-labeled probes (Shwartz and Zelzer, 2014). Probes are listed in Table S1. For analysis of *Shh-GFPCre*$^{-/-}$ mice, only mutants in which enthesis integrity was preserved were used.

For immunofluorescence staining, 10-µm-thick cryosections were air-dried for 1 h before staining. For IHH staining, sections were washed 2× in PBS+0.05% Tween-100 (PBST) for 5 min and blocked to prevent non-specific binding with 7% goat serum and 1% bovine serum albumin (BSA) dissolved in PBST. Then, sections were incubated with rabbit anti-IHH antibody (Abcam, AB39364, 1:50) at 4°C overnight. The next day, sections were washed 2× in PBST and incubated for 1 h with Cy2-conjugated fluorescent antibody (Jackson Laboratory, 711-225-152, 1:100). Slides were mounted with Immu-mount aqueous-based mounting medium (Thermo Fisher Scientific).

For Gli1 staining, 10-µm-thick cryosections were air dried for 1 h and fixed in 4% PFA for 10 min. Then, sections were washed 2× in PBST and endogenous peroxidase was quenched using 3% H_2O_2 in PBS. Next, antigen

Development (2018) 145, dev165381. doi:10.1242/dev.165381

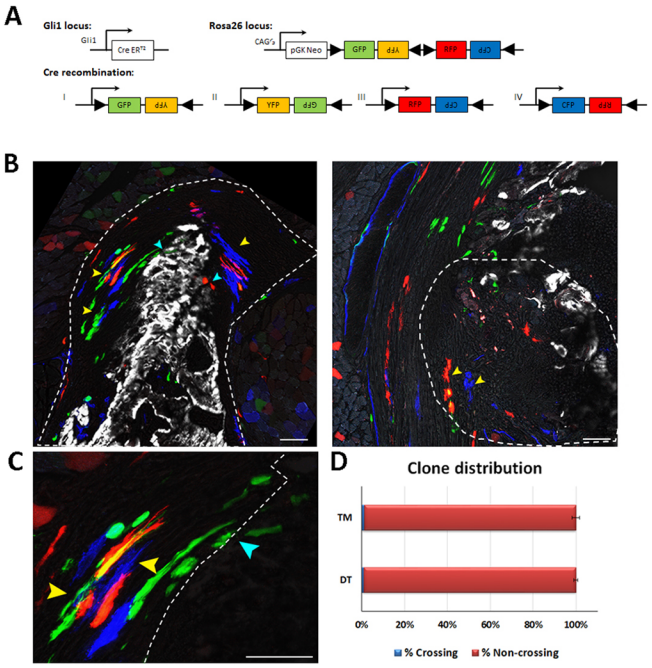

Fig. 10. *Gli1*$^{+}$ enthesis progenitors are compartmentalized during embryogenesis. Pulse-chase cell lineage experiments using *Gli1-CreERT2; R26R-Confetti* mice, in which *Gli1*$^{+}$ progenitor cell clones were labeled. *Gli1*$^{+}$ cells were labeled by a single tamoxifen administration at E13.5 and their descendants were followed to P14. One hour before sacrifice, mice were injected with Calcein Blue to mark mineralized tissue. (A) Schematic of possible Cre recombination outcomes. (B) Multiple clones were identified in the DT enthesis; however, the clones were restricted to either fibrocartilage or mineralized fibrocartilage and did not cross the border between the layers (yellow arrowheads). Cyan arrowheads indicate clones that crossed the border between the layers. The clones identified in the TM enthesis were restricted to the fibrous part and did not penetrate the bone. Dashed line demarcates the enthesis. (C) Magnification of DT clones in B showing crossing (cyan arrowheads) and non-crossing clones (yellow arrowheads). Dashed line marks the mineralization border. (D) Only a small percentage of identified *Gli1*$^{+}$ clones crossed the mineralization border in the DT (1.09%±0.9) and in the TM (1.22%±1.725). Scale bars: 50 µm.

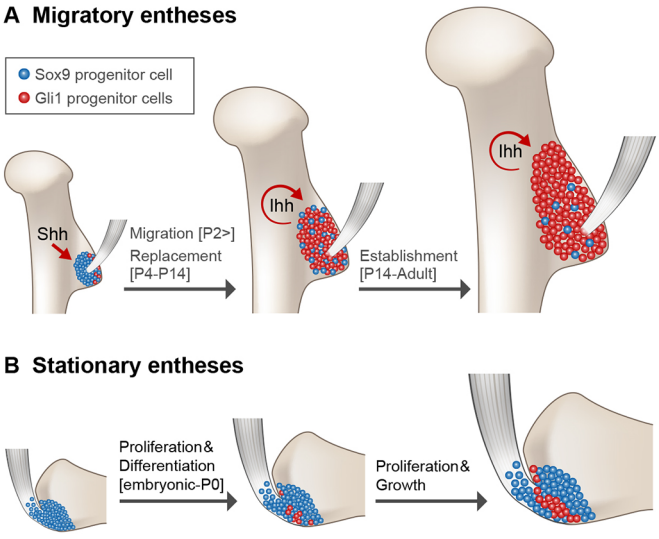

Fig. 11. Migrating entheses develop through template replacement. (A-B) Schematic of the developmental sequence of migratory and stationary entheses. During embryogenesis, *Sox9* lineage cells form an enthesis template. (A) In migrating entheses, *Sox9* lineage cells are replaced by a second population of *Gli1* lineage cells, which eventually form the mature enthesis. Specification of *Gli1* lineage is regulated by SHH, whereas maintenance of this population is regulated by IHH. (B) In stationary entheses, embryonic *Sox9* lineage cells proliferate and differentiate and, eventually, populate the postnatal enthesis structure. During late embryonic development, some *Sox9* lineage cells start expressing *Gli1*.

retrieval was performed using 0.3% Triton in PBS. Non-specific binding was blocked using 7% horse serum and 1% BSA dissolved in PBST for 1 h. Then, sections were incubated with Goat anti-GLI1 antibody (R&D Systems, AF3455, 1:100) overnight at room temperature. The next day, sections were washed 2× in PBST and incubated with Biotin anti-goat (Jackson Laboratory, 705065147, 1:100) for 1 h and then with streptavidin-HRP (Perkin Elmer, NEL750001EA, 1:200) for 1 h. HRP was developed using a TSA amplification kit (Perkin Elmer, 1:100) for 20 min, counterstained with DAPI and mounted with Immu-mount aqueous- based mounting medium.

Physical position of entheses

For identification of enthesis physical position, 2-4 limb samples at stages E16.5-P14 were scanned *ex vivo* using iodine contrast agent to allow visualization of the soft tissue. DT and TM positions were identified manually, and their physical position along the bone was calculated as described previously (Stern et al., 2015).

Cell lineage analysis

Tamoxifen (Sigma-Aldrich, T-5648) was dissolved in corn oil (Sigma-Aldrich, C-8267) at a final concentration of 5 mg/ml. Time-mated *R26R-tdTomato* females were administered 1 mg of tamoxifen by oral gavage (Fine Science Tools) at designated time points as indicated.

Cell count

For each age, two to four limbs from different litters were harvested, embedded in optimal cutting temperature compound (OCT) and sectioned at a thickness of 10 µm. Sections were imaged using a Zeiss LSM 780 microscope approximately every 80 µm, capturing red and DAPI channels. Images were then processed in ImageJ according to the following protocol. Each image was converted to an RGB stack and the region of interest was manually identified and cropped. Then, image levels were adjusted to improve separation between nuclei. A binary threshold was set automatically and conjoined nuclei were automatically separated using the binary watershed function. Using a home-made Matlab script, the number of nuclei was counted. Each nucleus that was co-localized with a red channel signal was counted as a tdTomato^{+} cell. For each section, the percentage of tdTomato^{+} cells was calculated and the average percentage of these cells was calculated for each bone. From each genotype and for each age group, at least three individual bones were sampled, and nine to 17 sections per bone were analyzed, depending on bone length. Statistical significance, defined as $P<0.05$, was determined using two-way ANOVA.

Fate mapping Confetti experiment

Tamoxifen was dissolved in corn oil at a final concentration of 20 mg/ml. Time-mated *R26R-Confetti* females were administered 4 mg of tamoxifen by oral gavage at E13.5. Cre^{+} pups were sacrificed at P14. Each pup was injected with Calcein Blue (Sigma, #m1255; 30 mg/kg) 1 h before sacrifice. Limbs were harvested, fixed for 30 min in 4% PFA at 4°C, embedded in OCT and sectioned at a thickness of 10 µm. Sections were imaged using a Zeiss LSM 780 microscope approximately every 80 µm.

Microscope settings and image analysis

At least 1024×1024 pixel, 8-bit images were acquired using the ×20 lens. A *z*-stack of two to four images was taken from each section. To detect GFP and YFP, the argon laser 488 nm was used. For RFP detection, a red diode laser emitting at 561 nm was used, and blue mCFP was excited using a laser line at 458 nm. Calcein Blue staining was detected using the 405 nm laser line. GFP fluorescence was collected between ~500-598 nm, Airy 1; RFP fluorescence was collected between ~606-654 nm, Airy 1; mCFP fluorescence was collected between ~464-500 nm, Airy 1 and Calcein Blue was collected between ~410-451 nm. For each image, a corresponding bright-field image was captured. The acquired images were processed using Photoshop and ImageJ.

To calculate the percentage of *Gli1*$^{+}$ clones found in both mineralized and non-mineralized fibrocartilage, the border between the zones was identified using the Calcein Blue signal. Clones that crossed the mineral border were manually counted and their percentage was calculated first for each section, then for each limb and, finally, for each type of enthesis. Data are presented as mean±s.d.

Acknowledgements
We thank Nitzan Konstantin for expert editorial assistance, Dr Ron Rotkoff for his help with statistical analysis and Dr Patrick Tschopp from the Clifford J. Tabin Lab at the Harvard Medical School for his assistance in generating *Shh* KO mice. Special thanks to all members of the Zelzer Laboratory for encouragement and advice.

Competing interests
The authors declare no competing or financial interests.

Author contributions
Conceptualization: N.F., E.Z.; Software: T.S.; Formal analysis: N.F., T.S.; Investigation: N.F.; Resources: S.R., S.K., D.P., B.A.P., R.S.; Writing - original draft: N.F., E.Z.; Writing - review & editing: N.F., E.Z.; Visualization: N.F.; Supervision: E.Z.; Project administration: E.Z.; Funding acquisition: E.Z.

Funding
This study was supported by grants from the National Institutes of Health (R01 AR055580) and the European Research Council (310098, and Proof of Concept grant 737473). It was also supported by the Weizmann Institute of Science, through the following funders: the Jeanne and Joseph Nissim Foundation for Life Sciences Research, the Y. Leon Benoziyo Institute for Molecular Medicine, Beth Rom-Rymer, the Estate of David Levinson, the Bernard M. and Audrey Jaffe Foundation, the Georges Lustgarten Cancer Research Fund, the David and Fela Shapell Family Center for Genetic Disorders, the David and Fela Shapell Family Foundation INCPM Fund for Preclinical Studies, and the Estate of Bernard Bishin for the Weizmann Institute of Science-Clalit Program. Deposited in PMC for release after 12 months.

Supplementary information
Supplementary information available online at
http://dev.biologists.org/lookup/doi/10.1242/dev.165381.supplemental

References

Ahn, S. and Joyner, A. L. (2004). Dynamic changes in the response of cells to positive hedgehog signaling during mouse limb patterning. *Cell* **118**, 505-516.
Akiyama, H., Kim, J.-E., Nakashima, K., Balmes, G., Iwai, N., Deng, J. M., Zhang, Z., Martin, J. F., Behringer, R. R., Nakamura, T. et al. (2005). Osteo-chondroprogenitor cells are derived from Sox9 expressing precursors. *Proc. Natl. Acad. Sci. USA* **102**, 14665-14670.
Benjamin, M. and McGonagle, D. (2009). Entheses: tendon and ligament attachment sites. *Scand. J. Med. Sci. Sports* **19**, 520-527.
Benjamin, M., Kumai, T., Milz, S., Boszczyk, B. M., Boszczyk, A. A. and Ralphs, J. R. (2002). The skeletal attachment of tendons–tendon "entheses". *Comp. Biochem. Physiol. A. Mol. Integr. Physiol.* **133**, 931-945.
Benjamin, M., Toumi, H., Ralphs, J. R., Bydder, G., Best, T. M. and Milz, S. (2006). Where tendons and ligaments meet bone: attachment sites ('entheses') in relation to exercise and/or mechanical load. *J. Anat.* **208**, 471-490.
Blitz, E., Sharir, A., Akiyama, H. and Zelzer, E. (2013). Tendon-bone attachment unit is formed modularly by a distinct pool of Scx- and Sox9-positive progenitors. *Development* **140**, 2680-2690.
Breidenbach, A. P., Aschbacher-Smith, L., Lu, Y., Dyment, N. A., Liu, C.-F., Liu, H., Wylie, C., Rao, M., Shearn, J. T., Rowe, D. W. et al. (2015). Ablating Hedgehog signaling in tenocytes during development impairs biomechanics and matrix organization of the adult murine patellar tendon enthesis. *J. Orthop. Res.* **33**, 1142-1151.
Buckingham, M., Bajard, L., Chang, T., Daubas, P., Hadchouel, J., Meilhac, S., Montarras, D., Rocancourt, D. and Relaix, F. (2003). The formation of skeletal muscle: from somite to limb. *J. Anat.* **202**, 59-68.
Dörfl, J. (1980a). Migration of tendinous insertions. I. Cause and mechanism. *J. Anat.* **131**, 179-195.
Dörfl, J. (1980b). Migration of tendinous insertions. II. Experimental modifications. *J. Anat.* **131**, 229-237.
Doschak, M. R. and Zernicke, R. F. (2005). Structure, function and adaptation of bone-tendon and bone-ligament complexes. *J. Musculoskelet. Neuronal Interact.* **5**, 35-40.
Dyment, N. A., Breidenbach, A. P., Schwartz, A. G., Russell, R. P., Aschbacher-Smith, L., Liu, H., Hagiwara, Y., Jiang, R., Thomopoulos, S., Butler, D. L. et al. (2015). Gdf5 progenitors give rise to fibrocartilage cells that mineralize via hedgehog signaling to form the zonal enthesis. *Dev. Biol.* **405**, 1-12.
Galatz, L., Rothermich, S., VanderPloeg, K., Petersen, B., Sandell, L. and Thomopoulos, S. (2007). Development of the supraspinatus tendon-to-bone insertion: localized expression of extracellular matrix and growth factor genes. *J. Orthop. Res.* **25**, 1621-1628.
Harfe, B. D., Scherz, P. J., Nissim, S., Tian, H., McMahon, A. P. and Tabin, C. J. (2004). Evidence for an expansion-based temporal Shh gradient in specifying vertebrate digit identities. *Cell* **118**, 517-528.
Kronenberg, H. M. (2003). Developmental regulation of the growth plate. *Nature* **423**, 332-336.
Liu, C.-F., Aschbacher-Smith, L., Barthelery, N. J., Dyment, N., Butler, D. and Wylie, C. (2012). Spatial and temporal expression of molecular markers and cell signals during normal development of the mouse patellar tendon. *Tissue Eng. Part A* **18**, 598-608.
Liu, C.-F., Breidenbach, A., Aschbacher-Smith, L., Butler, D. and Wylie, C. (2013). A role for Hedgehog signaling in the differentiation of the insertion site of the patellar tendon in the mouse. *PLoS ONE* **8**, e65411.
Logan, M., Martin, J. F., Nagy, A., Lobe, C., Olson, E. N. and Tabin, C. J. (2002). Expression of Cre recombinase in the developing mouse limb bud driven by a *Prxl* enhancer. *Genesis* **33**, 77-80.
Madisen, L., Zwingman, T. A., Sunkin, S. M., Oh, S. W., Zariwala, H. A., Gu, H., Ng, L. L., Palmiter, R. D., Hawrylycz, M. J., Jones, A. R. et al. (2010). A robust and high-throughput Cre reporting and characterization system for the whole mouse brain. *Nat. Neurosci.* **13**, 133-140.
Polly, P. D. (2007). Limbs in mammalian evolution. In *Fins into Limbs: Evolution, Development, and Transformation* (ed B. K. Hall), pp. 245-268. University of Chicago Press.
Razzaque, M. S., Soegiarto, D. W., Chang, D., Long, F. and Lanske, B. (2005). Conditional deletion of Indian hedgehog from collagen type 2α1-expressing cells results in abnormal endochondral bone formation. *J. Pathol.* **207**, 453-461.
Salton, J. A. and Sargis, E. J. (2009). Evolutionary morphology of the tenrecoidea (Mammalia) hindlimb skeleton. *J. Morphol.* **270**, 367-387.
Schwartz, A. G., Long, F. and Thomopoulos, S. (2015). Enthesis fibrocartilage cells originate from a population of Hedgehog-responsive cells modulated by the loading environment. *Development* **142**, 196-206.
Schwartz, A. G., Galatz, L. M. and Thomopoulos, S. (2017). Enthesis regeneration: a role for Gli1+ progenitor cells. *Development* **144**, 1159-1164.
Schweitzer, R., Chyung, J. H., Murtaugh, L. C., Brent, A. E., Rosen, V., Olson, E. N., Lassar, A. and Tabin, C. J. (2001). Analysis of the tendon cell fate using Scleraxis, a specific marker for tendons and ligaments. *Development* **128**, 3855-3866.
Shaw, H. M. and Benjamin, M. (2007). Structure-function relationships of entheses in relation to mechanical load and exercise. *Scand. J. Med. Sci. Sports* **17**, 303-315.
Shwartz, Y. and Zelzer, E. (2014). Nonradioactive in situ hybridization on skeletal tissue sections. *Methods Mol. Biol.* **1130**, 203-215.
Shwartz, Y., Viukov, S., Krief, S. and Zelzer, E. (2016). Joint development involves a continuous influx of Gdf5-positive cells. *Cell Rep.* **15**, 2577-2587.
Snippert, H. J., van der Flier, L. G., Sato, T., van Es, J. H., van den Born, M., Kroon-Veenboer, C., Barker, N., Klein, A. M., van Rheenen, J., Simons, B. D. et al. (2010). Intestinal crypt homeostasis results from neutral competition between symmetrically dividing Lgr5 stem cells. *Cell* **143**, 134-144.
Soeda, T., Deng, J. M., de Crombrugghe, B., Behringer, R. R., Nakamura, T. and Akiyama, H. (2010). Sox9-expressing precursors are the cellular origin of the cruciate ligament of the knee joint and the limb tendons. *Genesis* **48**, 635-644.
Stern, T., Aviram, R., Rot, C., Galili, T., Sharir, A., Kalish Achrai, N., Keller, Y., Shahar, R. and Zelzer, E. (2015). Isometric scaling in developing long bones is achieved by an optimal epiphyseal growth balance. *PLoS Biol.* **13**, e1002212.
Sugimoto, Y., Takimoto, A., Akiyama, H., Kist, R., Scherer, G., Nakamura, T., Hiraki, Y. and Shukunami, C. (2013). Scx+/Sox9+ progenitors contribute to the establishment of the junction between cartilage and tendon/ligament. *Development* **140**, 2280-2288.
Trainor, P. and Krumlauf, R. (2000). Plasticity in mouse neural crest cells reveals a new patterning rolefor cranial mesoderm. *Nat. Cell Biol.* **2**, 96-102.
Vortkamp, A., Lee, K., Lanske, B., Segre, G. V., Kronenberg, H. M. and Tabin, C. J. (1996). Regulation of rate of cartilage differentiation by Indian Hedgehog and PTH-related protein. *Science* **273**, 613-622.
Wang, M., Vanhouten, J. N., Nasiri, A. R., Johnson, R. L. and Broadus, A. E. (2013). PTHrP regulates the modeling of cortical bone surfaces at fibrous insertion sites during growth. *J. Bone Miner. Res.* **28**, 598-607.

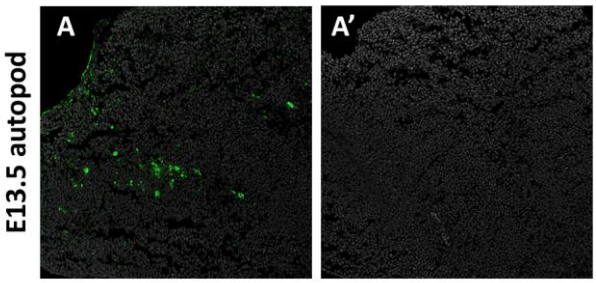

Figure S1. TUNEL staining control

E13.5 mouse autopod was used as a control for TUNEL staining in Figure 8. Cells positive for TUNEL staining appear green. A, positive control; A', negative control without enzyme.

Table S1. *In situ* hybridization probes

Probe name	Genomic position	Ref-seq template	Size
Col1a1	4295 to 4475	NM_007742.4	180 bp
Col2a1	4474 to 4879	NM_001113515.2	406 bp
BSP	145 to 1058	NM_008318.3	1955 bp
Col12a1	8103 to 8771	NM_001290308.1	689 bp
*Tnc**	484 to 1118	NM_011607.3	635 bp
Gli1	1810 to 2427	NM_010296.2	638 bp

* Tnc plasmid was kindly contributed by Professor Murizio Pacifici, Children's Hospital of Philadelphia